Thermite additive manufacturing feedstocks

S. M. La Vars[1], M. G. Morgan[1], J. S. Brusnahan[1]*

[1]Defence Science and Technology Group
P.O. Box 1500, Edinburgh, SA 5111, Australia
*email: jasonstewart.brusnahan@dst.defence.gov.au

Abstract:
Thermites are mixtures of metals and metal oxides that are traditionally valued for their high reaction temperature, low gas production, molten solid reaction products and low explosive sensitiveness. This makes these formulations ideal for cutting, welding, and incendiary devices that require controllable burn rates and optimum heat production. Traditional thermites are used in powdered or block form. This requirement limits the geometry of thermite charges and can restrict their application. The pressing of thermite blocks is a process that has inherent hazards, and the final products can have mechanical or ignition failures, especially when multiple blocks are required to produce the desired effect (e.g. variable burn rates). A potential means of overcoming the geometric limitations and hazards associated with the production and handling of traditional thermite formulations is to employ additive manufacturing (AM). AM represents a means of producing energetic materials with bespoke, multi-material charge geometries that offer tailored energy release, improved safety and handling as well as on-demand production. Complex three-dimensional architectures can be obtained by the sequential layering of energetic material via extrusion-based additive manufacturing technologies, but the successful use of such AM techniques requires the development of thermite feedstocks that are compatible with the printer technology in question. This paper provides outcomes of initial AM-compatible thermite feedstock development research centred on satisfying ingredient compatibility and safe handling and processing whilst meeting nominal performance requirements. Results will be presented for traditional copper(II) oxide (CuO)/aluminium and bismuth(III) oxide (Bi_2O_3)/aluminium powder-based thermites and these will be compared with solvent-based, binder-containing feedstocks that employ the same fuel-oxidiser constituents, with identical stoichiometry and that are suitable for extrusion-based AM.

Keywords: thermite, additive manufacturing, extrusion, sensitiveness, simultaneous differential thermal analysis

---

1. Introduction

Thermite compositions are reactive mixtures that consist of a metal oxide and a metal. Traditional thermites are mixtures of iron oxide and aluminium; however thermites can be prepared using other metals (e.g. magnesium, titanium) and a range of metal oxides (e.g. copper(II), bismuth(III), molybdenum(VI), manganese(II), chromium(III), lead(II, IV) oxides) depending on the desired pyrotechnic effect [1-3]. Thermites are typically used in applications that require a high concentration of heat, little to no gas production, the formation of solid reaction products, controlled burn rate that is independent of ambient pressure (e.g. underwater or in space), and insensitiveness to most ignition stimuli [1-3]. Common applications for thermite compositions are pyrotechnic devices for cutting, welding, and perforating, as well as incendiary devices [2]. Traditionally, due to the limitations of current production methods, thermites are used in powdered or block form. This limits the geometry of thermite charges and can restrict their application. For instance aluminium thermites do not press well and can be prone to both mechanical and ignition failures, especially when multiple blocks are required to produce the desired effect (e.g. variable burn rates) [1-3]. Recently, there has been a strong interest in the additive manufacturing (AM) of energetic materials to realise bespoke three-dimensional architectures that can improve their performance (e.g. propellants) and broaden their operational flexibility [4]. Similarly, the use of AM technologies in the production of thermites offers a potential means to overcome some of the current limitations of traditional thermites. These thermite AM feedstocks can allow compositions to be produced in novel architectures at low cost, and the tailoring of energy outputs through these architectures, whereas traditionally one had to rely on changing the formulation to meet new energy

requirements. Other advantages of the AM of thermites are in the improved safety and handling characteristics of energetic AM feedstocks in comparison to traditional production methods. This technology enables remote production and *in situ* mixing of ingredients, reducing operator contact with the thermite, and removes the need to press loose powders. Inert feedstocks can also be prepared and combined at the point of printing, eliminating the need to store and transport energetic material. However, to achieve this will require the identification of suitable AM technologies and the development of AM-suitable feedstocks.

Current AM technology is divisible into seven main categories; material extrusion, vat photopolymerisation, material jetting, binder jetting, sheet lamination, powder bed fusion and direct energy deposition [5-8]. Not all of these techniques are suitable for use with energetic materials, with the directed energy deposition and powder bed fusion categories being particularly ill-suited due to higher energy requirements and greater potential for accidental ignition.

Material extrusion, which encompasses techniques such as fused deposition modelling (FDM) and direct ink writing (DIW), is of particular interest as an AM technology as it allows for great flexibility in feedstock materials; solid filaments, powders, pastes and inks [6, 7] and achievable multi-material architectures. Material extrusion AM consists of moving material through a nozzle onto a build platform, building three-dimensional structures layer-by-layer. The advantages of material extrusion over other technologies include low cost, geometric consistency, a wide variety of available binders, and lower quantities of energetic material feedstocks required for a given object compared to other AM technologies [5, 9].

This work describes the development of suitable thermite feedstocks for use with extrusion based AM technologies. The ignition sensitiveness of these thermite AM feedstocks were compared to traditional thermite compositions, the chemical compatibility of the ingredients was determined, and the impact of feedstock formulation on the pyrotechnic output was also examined.

2. Materials and Methods

2.1. Materials

It should be noted that pyrotechnic compositions are highly energetic and that suitable safety precautions must be employed when working with them to minimise the likelihood of inadvertent ignition. The reagent grade ingredients used to produce thermite mixtures were copper(II) oxide (CuO) (Sigma-Aldrich), bismuth(III) oxide (Bi_2O_3) (Sigma-Aldrich), and Standart Pyro 5413 H Super aluminium (Al) powder (ResChem Technologies). The thermoplastics polymethyl methacrylate (PMMA) and polylactic acid (PLA) (Sigma-Aldrich, Australia) were employed as the AM binder. Dichloromethane (Bio-Strategy) was selected as an appropriate solvent for this investigation.

2.2. Thermite Preparation

After drying the thermite ingredients overnight at 100 °C, a maximum of 10 g of each composition was prepared by weighing out the ingredients required for each formulation and fully combining the thermite ingredients using a WAB Turbula mixer (50 rpm for 20 minutes). Both inert and thermite AM formulations were produced by pre-dissolving the selected binder in a minimal amount of dichloromethane. The thermite or inert solids were then hand mixed with the pre-dissolved binder solution. The feedstocks were allowed to cure by evaporation of the solvent under ambient conditions. Initially, formulations consisting of binders and individual thermite ingredients were qualitatively assessed for structural integrity and homogeneity before proceeding to the production of thermite compositions. The properties of the cured inert formulations were visually inspected for testing as potential energetic AM feedstock.

2.3. Modelling

Thermodynamic equilibrium calculations were performed on the binary thermite formulations with FactSage 7.0 (Thermfact/CRCT and GTT-Technologies) [10]. The particular databases used were FactPS, FToxid, and a custom database containing thermodynamic data for CuO, Bi_2O_3, and Al. The custom database was professionally built by The Spencer Group, Inc. using available literature data [10]. All simulations assumed a constant pressure of 1 atm with the reactants initially at 298.15 K. The analyses were performed in adiabatic mode ($\Delta H = 0$). The results consist of predicted adiabatic reaction temperatures (T_{ad}) and the thermodynamic products at those temperatures. Possible thermodynamic equilibrium products included neutral species in the gas, liquid, and solid phases.

2.4. Characterisation

Scanning electron microscope (SEM) images of the thermite ingredients were captured using an FEI Inspect F50 SEM. Particle sizing was

performed using a Mastersizer 2000, with water as the dispersant. Initial flame ignition testing was achieved through the application of a burning safety match to 0.5-1.0 g of the thermite AM formulations deposited on a square of aluminium foil. This initial attempt was followed by application of a MAPP gas blowtorch if match ignition failed. All still and video images were captured using a Sony Alpha (SLTA58) DSLR camera. Post processing of the videos was undertaken utilising Windows Live Movie Maker (Version 2011, Build 15.4.3555.0308) by Microsoft Corporation (2010).

Sensitiveness data was measured in accordance with established protocols [11]. Friction sensitiveness was measured using a Julius Peters BAM friction apparatus and the values reported represent the lowest setting at which a 10 mg sample initiated; 6 repetitions of the experiment at the next lower setting produced nil initiations. Sensitiveness to impact was determined utilising a Rotter Impact apparatus (DST Group). The experiment was repeated 25 times utilising 30 mg samples with a standard drop weight of 5 kg and the reported values for Figure of Insensitiveness (F of I) were standardised to RDX (F of I = 80). A 'go' event was determined via visual inspection of the rotter caps indicating a colour change, presence of charring and/or smoke. Temperature of Ignition (T of I) was determined utilising 200 mg samples heated (in duplicate) at 5 °C/min to a maximum temperature of 400 °C within a shielded heating block. Sensitiveness to electrostatic discharge (ESD) was measured by passing electrical discharges of 4.5 J, 0.45 J and 0.045 J through ≈ 10 mg samples utilising purpose-built equipment (DST Group).

Chemical compatibility of the various ingredients was examined using both Pressure Vacuum Stability Test (PVST) analysis (TNO and Tamson Instruments TC 16) and Simultaneous Differential Thermal (SDT) analysis (TA Instruments, Q600). Duplicate samples consisting of neat binder and thermite ingredients and 1:1 mixture by weight of each ingredient combination were prepared. For PVST, each sample was placed into an evacuated test tube in a water bath at 100 °C for 48 hours. The stabilised pressure inside the test tubes was measured before and after the heating process, and the amount of gas per gram of material was calculated. The amount of gas per 5 g of mixture was then compared to the amount of gas per 2.5 g of neat ingredient. Less than 5 mL of gas produced by any reaction between the ingredients indicates the ingredients are compatible. For SDT analysis, a total mass of 3-7 mg of each sample was heated in an alumina pan at 10 °C/min to a final temperature of 600 °C, under a nitrogen atmosphere with a flow rate of 50 mL/min. A comparison was then made of the SDT curve features of the compositions and the neat ingredient control samples. Chemical compatibility was determined by the degree to which the thermal features of the composition trace differed from the control. The tolerances for chemical compatibility are as follows: A difference of <4 °C indicates chemical compatibility, a difference of between 4-20 °C indicates a degree of chemical incompatibility, and a difference of >20 °C indicates chemical incompatibility [12].

3. Results and Discussion

3.1. Modelling

To determine the weight ratios of each oxidiser and aluminium required for optimum thermite performance, thermodynamic modelling was conducted using the FactSage 7.0 software. The plots for potential CuO/Al and Bi_2O_3/Al thermite reactions are shown in Figure 1.

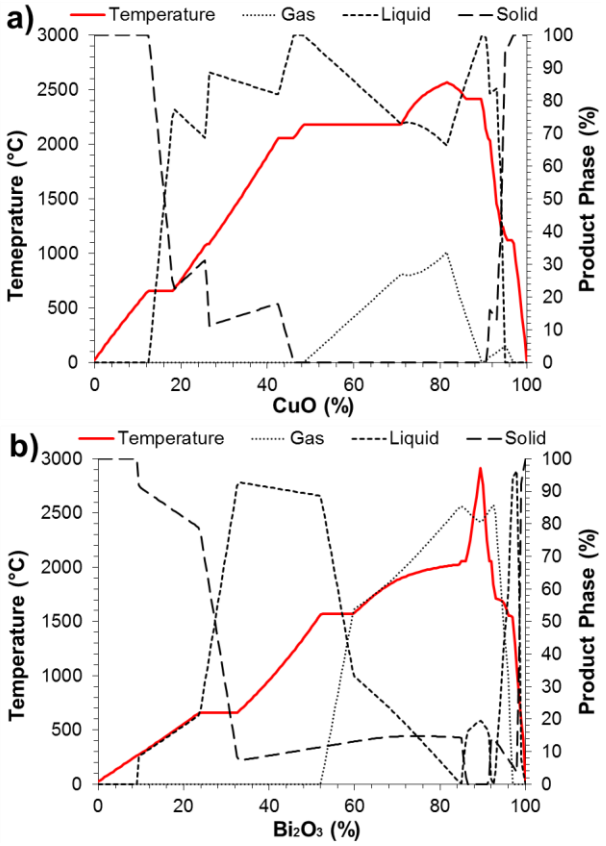

Figure 1: FactSage plot of reaction temperature and amount of product by phase against oxidiser content (wt%) of CuO/Al (a) and Bi_2O_3/Al (b) thermites

The desired pyrotechnic effect may be obtained by maximising temperature output, or amount of gaseous or liquid products. For instance, cutting

applications may require a high reaction temperature, while thermite welding or rock-breaking may require the production of molten or gaseous products, respectively. The FactSage modelling predicted the maximum adiabatic flame temperature and reaction products, including their physical state (solid, liquid, gas) for a range of possible oxidiser wt% values.

The thermodynamic modelling suggests the maximum possible temperatures produced by the CuO/Al and Bi_2O_3/Al thermite reactions are 2566 °C and 2917 °C, respectively. A summary of potential mix ratios suggested by the modelling to maximise temperature output, gaseous reaction products and liquid reaction products is presented in Table 1.

Table 1: Oxidiser wt% and predicted output of thermites with optimal temperature, gas and liquid production

	CuO		Bi_2O_3	
	Output	**(wt%)**	**Output**	**(wt%)**
Temp.	2566 °C	81	2917 °C	89.5
Gas	34%	81.5	86%	92.5
Liquid	100%	90	96%	98

As a result of the thermodynamic modelling, the ingredients were used to produce close to stoichiometric thermite compositions, as these ratios were determined to provide optimal performance through heat output, within a reasonable margin of error; CuO/Al (80:20 wt%) and Bi_2O_3/Al (90:10 wt%).

3.2. Thermite Ingredient Characterisation

As particle morphology and size can have a significant impact on pyrotechnic reaction rates [13], SEM images of the thermite ingredients were collected to characterise the particle shapes of the ingredients. Typical images of the Al, CuO and Bi_2O_3 particles are shown in Figure 2.

The super fine aluminium particles (Figure 2a) were found to be angular and flake-like in appearance. The CuO particles (Figure 2b) were also angular and irregular in shape; however the particles appear less flaky and more porous. The Bi_2O_3 particles were found to be significantly smoother, mostly spheroidal particles (Figure 2c), with some wire-like structures scattered throughout. These particles were also more likely to appear as aggregates, and as such, extra care had to be taken during mixing to ensure the final formulations were homogeneous. Both the CuO and Bi_2O_3 oxidisers were determined to have similar mean particles sizes of 6.7 µm and 6.3 µm, respectively. The Al mean particle size was found to be slightly larger at 10.9 µm.

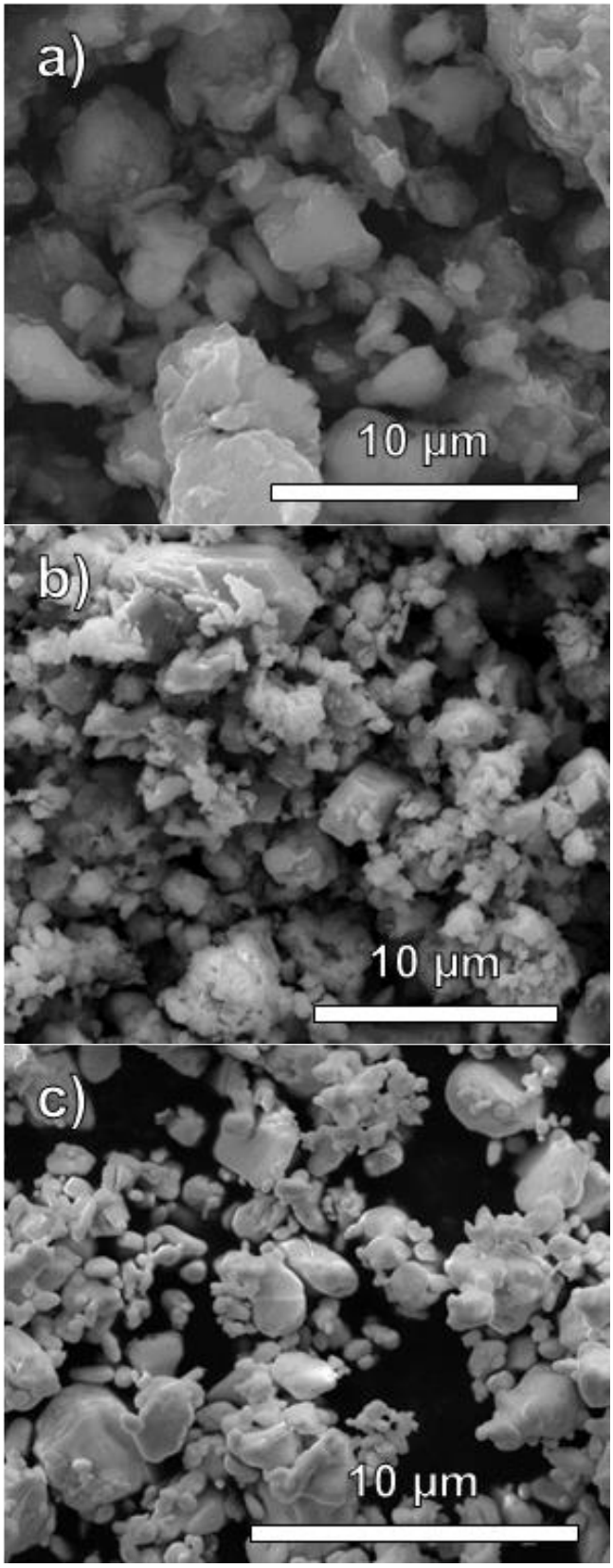

Figure 2: Typical SEM images of the thermite material used - a) super fine aluminium powder; b) copper(II) oxide powder; c) bismuth(III) oxide powder

Given their extensive use in AM, and desirable physical and mechanical properties the thermoplastics PMMA and PLA were selected as the AM binders to employ in this study [7, 14-16].

Dichloromethane has previously been used to successfully create highly solids loaded inks that have been utilised in the FDM of metal and metal oxides, and as such was chosen as an appropriate solvent for this work [17, 18]. Ideally, the amount of any solvent should be kept to a minimum in order to keep formulations as simple as possible and minimise other potential risks introduced by large quantities of toxic and/or flammable liquid or other chemical hazards.

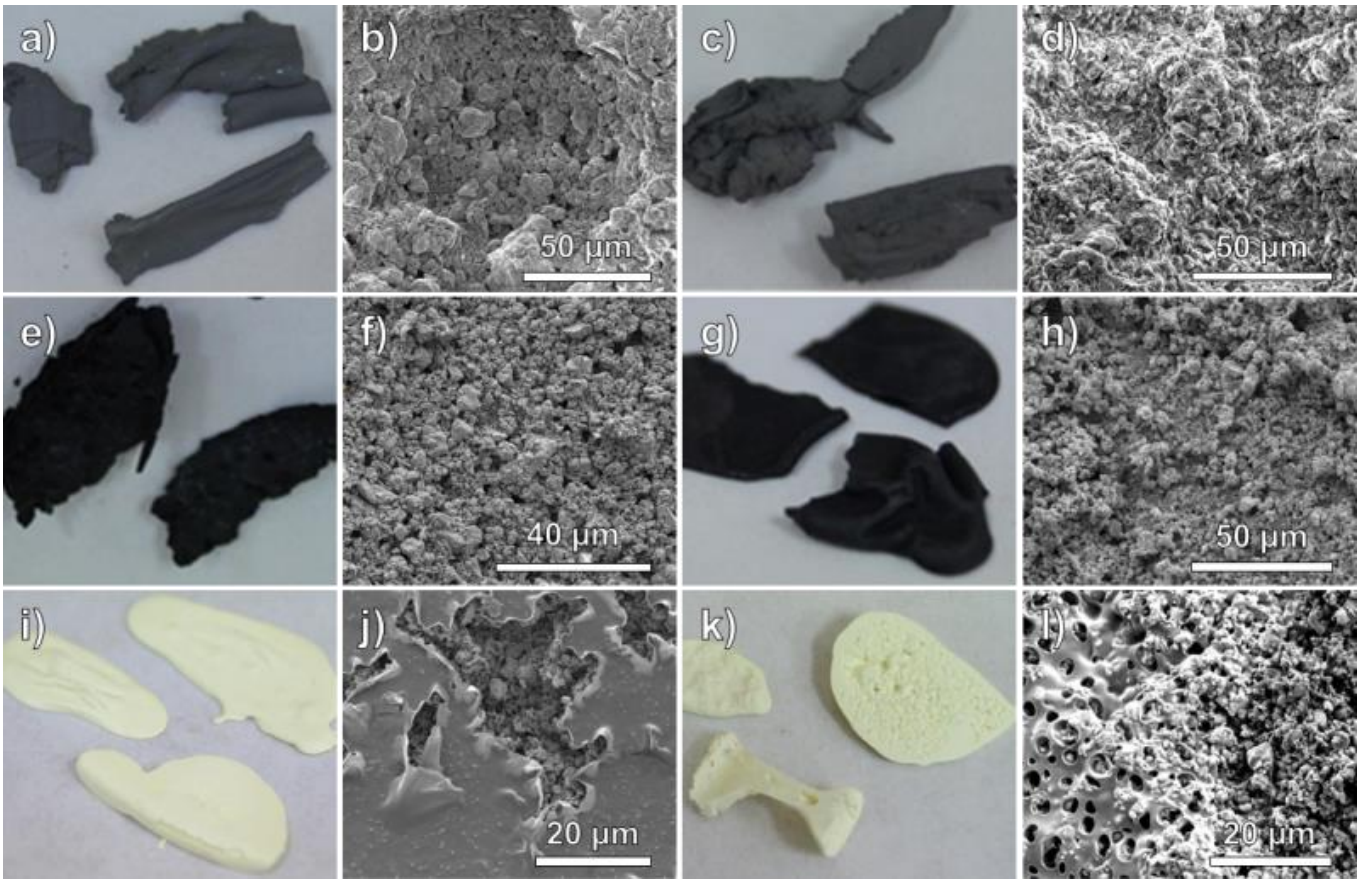

Figure 3: Photographs and SEM images of 90 wt% solids loaded inert AM formulations; Al in PMMA a-b) and PLA c-d); CuO in PMMA e-f) and PLA g-h); Bi_2O_3 in PMMA i-j) and PLA k-l)

3.3. Physical properties

Previous studies have demonstrated high solids-loading is required in pyrotechnic AM feedstocks to avoid the dilution of energetic output, which must be balanced against the rheological properties of the feedstock and mechanical requirements of the final cured material [19]. The preparation of inert feedstocks for point-of-printing energetic material production requires each component to be readily incorporated into binder matrices while maintaining mechanical strength at high solids loadings. As such, inert mixtures of each thermite ingredient (Al, CuO, and Bi_2O_3) with each binder (PLA and PMMA) at 90 wt% solids loading were prepared. These formulations were initially assessed for homogeneity and their mechanical properties qualitatively assessed by visual inspection and handling of the cured product. More rigorous testing of the mechanical properties of the final formulations will be required to precisely quantify the response of printed products to mechanical stresses. Images of the cured inert mixtures are shown in Figure 3.

All of the inert mixtures cured quickly due to the fast evaporation of dichloromethane under ambient conditions. Although homogeneous, the resulting PMMA/Al mixture (Figure 3a) was found to be brittle, and readily crumbled. The PLA/Al mixture (Figure 3c) was noticeably less brittle. The SEM images show the PMMA/Al mixture (Figure 3b) consists of large particulate agglomerates held together by the binder, while the SEM images of the PLA/Al mixture (Figure 3d) present smaller particles distributed evenly throughout the binder matrix to form a more homogeneous material. It is expected that the brittleness of the PMMA formulation may be mitigated in the final thermite AM formulation, as the Al content will ultimately be <30 wt%, allowing for higher proportions of binder in any inert feedstock prepared for point-of-printing applications. Future compositions requiring greater powdered aluminium content will need to

take this effect into consideration. The PMMA/CuO mixture (Figure 3e) appeared less homogeneous, with some sections of the cured material inclined to crumble, however the bulk of the material cured solid and hard. The SEM images of this formulation (Figure 3f) displayed similar particle distribution to the PMMA/Al mixture; particle agglomerates held together by the binder in a porous matrix.

The PLA/CuO mixture (Figure 3g) cured rigid and tough, suggesting this binder will readily incorporate high proportions of this ingredient while maintaining good mechanical strength. As can be seen in the SEM image (Figure 3h) the CuO appeared more fully incorporated in the PLA matrix, with the particles appearing to be homogeneously distributed through the material; however the structure was obviously more porous than the PLA/Al mixture. The PMMA/Bi_2O_3 mixture (Figure 3i) cured rigid and tough, with the SEM images showing the solid homogeneously distributed through the binder matrix in much the same manner as the other PMMA-based mixtures (Figure 3j). This mixture also resulted in the formation of a binder "skin" over some sections of the bulk material. This is consistent with the observations made during the curing process, with skin formation typically coinciding with fast evaporation of the solvent.

The PLA/Bi_2O_3 mixture exhibited agglomeration of Bi_2O_3 particles which appear to settle during cure, with loose powder and voids evident underneath the cured binder matrix (Figure 3k). The SEM images of this formulation (Figure 3l) reveal the PLA matrix, which in every other mixture appeared to evenly coat particles, in this instance appeared highly aerated and porous. This suggests potential chemical incompatibility between the Bi_2O_3 and PLA, resulting in the porous binder structure that is conspicuously absent in the other inert formulations.

3.4. Rheology

An initial qualitative assessment of the rheological properties of potential AM feedstocks was performed. The feedstocks consisted of a 7-9 vol% solids loading in dichloromethane, with solid ingredient ratios maintained at 10 wt% binder (PLA or PMMA) and 90 wt% oxidiser (CuO or Bi_2O_3).

For the feedstocks it was noted how readily the material extruded by hand through a 10 mL plastic syringe (internal tip diameter of 1.7 mm), in a serpentine pattern onto a glass slide. No significant clogging of the syringe tip was observed for the PLA/CuO, PLA/Bi_2O_3 and PMMA/Bi_2O_3 mixtures, and the resulting line spread was recorded by measuring the deposition at its thickest and thinnest points. Due to significant nozzle clogging, the PMMA/CuO mixture was unable to be assessed. The PLA/CuO and PLA/Bi_2O_3 mixtures both showed minimal spreading, with the thinnest and thickest line widths of 2 mm and 4 mm, respectively. The PMMA/Bi_2O_3 mixture showed much greater spreading, with the thinnest and thickest sections of the line measured at 3 mm and 5 mm, respectively.

Adhesion of the dry extruded product to the glass substrate was also assessed, with both PLA mixtures adhering well to the glass substrate, and the PMMA/Bi_2O_3 mixture displaying a tendency to crack and peel. Multi-layer structures were also produced by adding layers with a glass pipette to both 'lines' and 'dots' of material to observe if the material adhered to itself, and whether it developed a three-dimensional structure or simply spread further upon the slide. Each layer was allowed to dry prior to subsequent depositions. All mixtures were able to be layered to develop three-dimensional structure; however the PLA/Bi_2O_3 mixture showed signs of ingredient separation as the solvent evaporated.

Overall, the PLA/CuO feedstock exhibited positive rheological properties; however the Bi_2O_3 feedstocks exhibited some behaviour that will require further investigation such as greater spreading of material, separation of the oxidiser from the binder and curling and cracking as the solvent evaporated.

3.5. Chemical compatibility

The data provided by the various methods of chemical compatibility testing techniques is relative, and while they may each provide an indication of ingredient compatibility, the results are not absolute values. As such, a multi-faceted approach to chemical compatibility is taken, and reasonable caution should be exercised when determining the acceptability of the data.

3.5.1. Pressure vacuum stability test (PVST)

The volume of gas generated by any reaction between ingredients (V_R) in a mixture is calculated using the following equation:

$$V_R = M - (E + S)$$

Where M is the measured volume of gas evolved from 5 g of the 1:1 mixture, E is the measured

volume of gas evolved from 2.5 g of thermite ingredient, and S is the measured volume of gas evolved from 2.5 g of the polymeric binder. The V_R value must be less than 5 mL for two materials to be compatible, which is equivalent to 1 mL/g of gas produced by chemical reaction in addition to the gas evolved by each ingredient alone. The average gas evolved per gram of sample and calculated V_R values with associated standard deviations are shown in Table 2.

Table 2: Average gas production per gram as measured by PVST, and calculated volume of gas produced by ingredient reactions per 5 g of 1:1 mixture (V_R)

	Average gas production (mL/g)	V_R (mL)
Al	0.63	-
CuO	0.05	-
Bi_2O_3	0.02	-
PMMA	0.11	-
PLA	0.05	-
Al/PMMA	1.12	3.78 ± 0.28
Al/PLA	1.38	5.19 ± 0.71
CuO/PMMA	0.80	3.61 ± 0.20
CuO/PLA	1.00	4.75 ± 0.14
Bi_2O_3/PMMA	0.76	3.31 ± 0.12
Bi_2O_3/PLA	0.93	4.32 ± 0.58

The PVST of the control samples showed the average gas production by each neat thermite ingredient and binder was less than 1 mL. Most of the mixtures of thermite ingredients with the two binders resulted in significant V_R values of <5 mL. This suggests the majority of the thermite ingredients are chemically compatible with both the PLA and PMMA binders. The Al/PLA mixture is the exception, with this combination resulting in a V_R value of 5.19 mL. However, the error associated with this value encompasses the 5 mL threshold for compatibility set for PVST, suggesting further compatibility testing is required.

3.5.2. Simultaneous differential thermal (SDT) analysis

The SDT heat loss and weight loss curves of the neat thermite ingredients (CuO, Bi_2O_3 and Al) show no significant thermal or weight change events over the 600 °C temperature range, well past the temperature of decomposition of both PLA and PMMA. Examples of the heat flow and weight loss SDT curves of PMMA and 1:1 mixtures of PMMA with each thermite ingredient are shown in Figure 4.

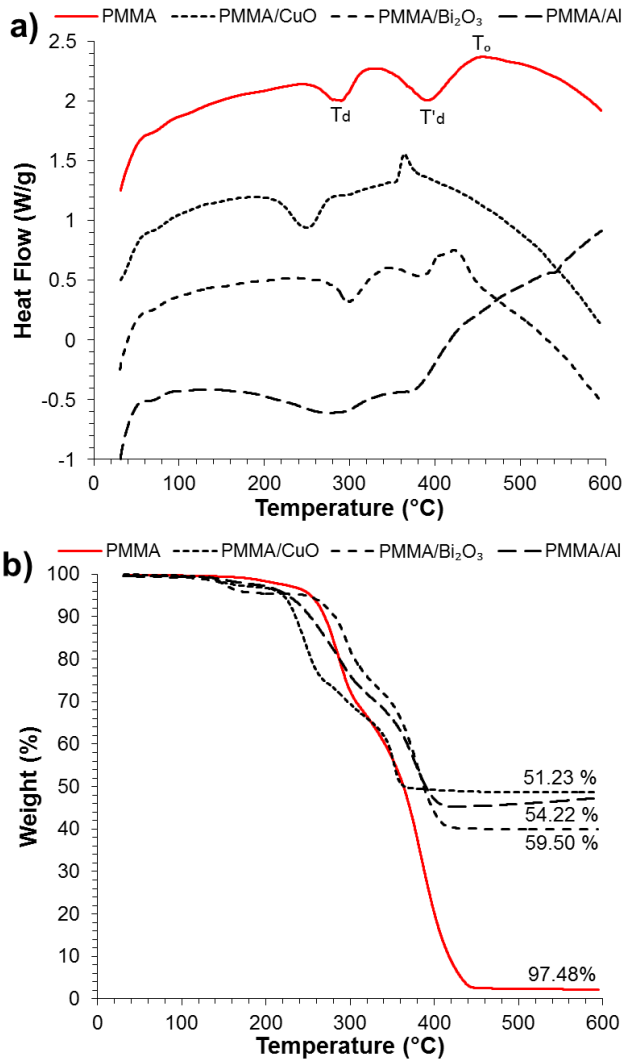

Figure 4: Example a) heat flow and b) weight loss SDT curves of PMMA, PMMA/CuO, PMMA/ Bi_2O_3, and PMMA/Al

Thermal PMMA decomposition is complicated, and the features observed during thermal analysis depend on the method of manufacture [21, 22]. The large variability in the type of polymerisation reactions and additives used during the manufacture of PMMA leads to large variability in the features of the thermal traces [21-24].

The PMMA heat flow curves consists of two distinct endothermic decomposition events at 250-300 °C and 350-400 °C, which agree with previously reported initiation of unsaturated polymer chain ends (T_d) and polymer backbone (T'_d), respectively [25]. The heat flow curves show no obvious thermal event to indicate head-to-head interactions decomposing, nor is there an obvious melting temperature in the expected 85-170 °C range [23]. The exothermic event seen at >400 °C (T_o) has been observed in the literature under inert atmosphere, with exothermic decomposition also shown to occur under oxygen atmosphere over

400 °C [26, 27]. This event is occurring in the gaseous phase, with the mass loss curves indicating the solid polymer has decomposed by this point, and is likely due to monomer or other gas-phase reaction product reactions or residual random chain scissions [21, 22, 27]. It is also possible that shifts in these events observed when the polymer is combined with the thermite ingredients may be due to interactions between these decomposition products and the solid thermite components [26].

Table 3: Average chemical compatibility of PMMA and PLA with thermite ingredients determined by SDT analysis (°C)

	T_m	ΔT_m	T_d	ΔT_d	T'_d	$\Delta T'_d$	T_o	ΔT_o
PMMA			288.5	-	391.0	-	451.7	-
PMMA/Bi_2O_3			297.4	8.8	386.2	-4.8	424.3	-27.4
PMMA/CuO			247.5	-41.1	299.7	-91.3	369.0	-82.6
PMMA/Al			292.3	3.8	377.9	-13.1	424.5	-27.2
PLA	145.6	-	345.6	-			374.6	-
PLA/Bi_2O_3	148.2	2.6	264.6	-81.0			377.4	2.8
PLA/CuO	148.7	3.1	340.6	-4.9			373.6	-1.0
PLA/Al	147.4	1.8	344.8	-0.7			384.9	10.3

The average temperatures of the thermal events observed in the heat flow curves of PMMA and PMMA mixtures are shown in Table 3. The negative values indicate a decrease in the temperature, while positive values indicate an increase in temperature of a thermal event. The Bi_2O_3 shows a degree of chemical incompatibility with the PMMA, causing a shift in the temperatures at which the decomposition events in the polymer are occurring, and significantly decreasing the temperature of the exothermic event observed in the gaseous phase post-decomposition by an average of -27.4 °C. The Al also shows a degree of chemical incompatibility, by a significant shift of an average of -13.1 °C in the second decomposition event compared to neat PMMA, and a similar decrease in the exothermic event temperature to the PMMA/Bi_2O_3 mixture. The CuO displays a large degree of chemical incompatibility with the PMMA, with >20 °C shifts in all thermal events. This may impact the suitability of PMMA as a binder for CuO/Al thermite mixes, indicating a potential decrease in chemical stability of the mixture that may reduce shelf-life. Although it does not eliminate PMMA as a binder, it does suggest further investigation into ageing and heating effects are required. The heat flow curve of PLA shows the melting point (T_m) and the decomposition temperature (T_d) of the polymer, with the decomposition occurring over the same temperature range at which the weight loss curve indicate a single mass reduction event. Similar to the PMMA traces, an exothermic event is observed occurring at >400 °C (T_o), past the point at which the weight loss traces indicate that the polymer has been consumed. This is also likely due to interactions between gaseous polymer decomposition products with each other and potentially with the thermite ingredients [22, 26]. Examples of the heat flow and weight loss SDT curves of PLA and 1:1 mixtures of PLA with the thermite ingredients are shown in Figure 5.

The average temperatures of the thermal events observed in the heat flow curves of PLA and PLA mixtures are shown in Table 3. The negative values indicate a decrease in the temperature, while positive values indicate an increase in temperature of a thermal event. The PLA/CuO trace displayed a degree of chemical incompatibility between these ingredients, as indicated by a small shift of up to 4.9 °C in the melting point and the decomposition temperature. The PLA/Bi_2O_3, however, displays pronounced chemical incompatibility, as evident by the significant shift of 81.0 °C in the decomposition event compared to neat PLA.

Overall, the CuO displays a much higher degree of chemical compatibility with the PLA binder compared to the PMMA, while the reverse is true for Bi_2O_3. The Al appears the most compatible with PLA, displaying a moderate degree of incompatibility with PMMA. These findings may translate to better performance and stability of formulations consisting of PLA/CuO/Al or PMMA/Bi_2O_3/Al.

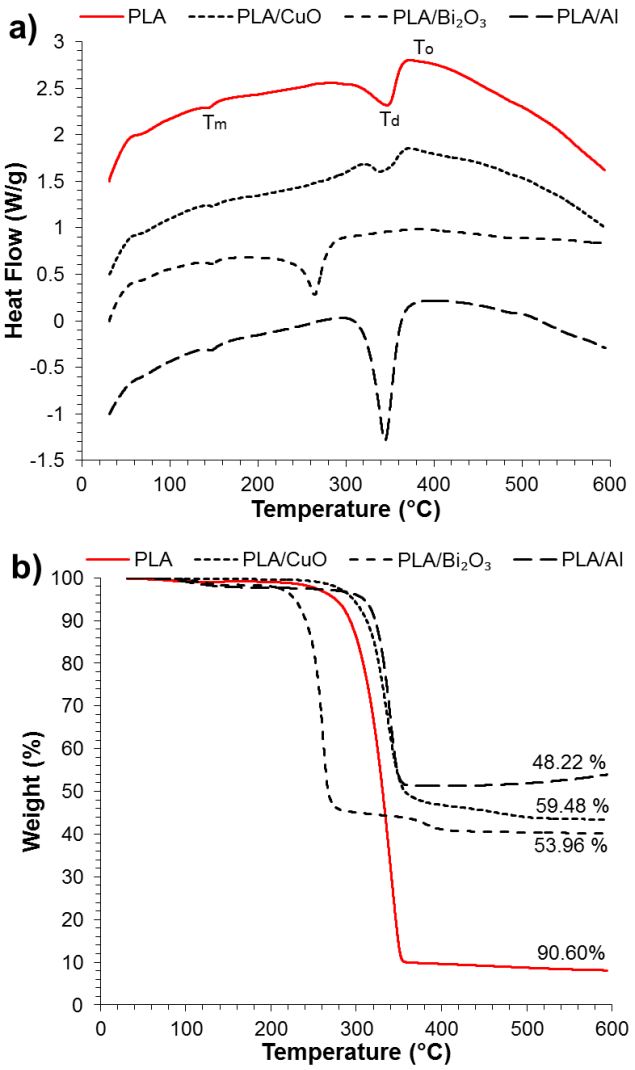

Figure 5: Example a) heat flow and b) weight loss SDT curves of PLA, PLA/CuO, PLA/Bi_2O_3, and PLA/Al

3.6. Sensitiveness

The sensitiveness properties of the neat stoichiometric thermite compositions and the AM thermite formulations are given in Table 4.

As expected, the traditional CuO/Al thermite exhibited high thermal stability with Temperature of Ignition (T of I) values greater than 400 °C and low sensitiveness to friction. This thermite composition exhibited moderate sensitiveness to impact. However, the CuO/Al thermite displays significant ignition sensitiveness to ESD, which is of concern from a safe handling perspective. Bi_2O_3/Al also exhibited a similarly high thermal stability, with T of I in excess of 400 °C. However, as was the case with the CuO/Al composition, the Bi_2O_3 displayed very high sensitiveness to ESD. This is coupled with a greater sensitiveness to friction, and almost double the F of I value compared to the CuO/Al composition. The FactSage modelling of the Bi_2O_3/Al thermite indicated that for a stoichiometric mix, 80% of the predicted reaction products would be in gaseous state; which is much greater than that predicted for the CuO/Al stoichiometric composition, at only 33%.

This was in agreement with observations during impact sensitiveness testing, with the average gas output of the Bi_2O_3/Al composition approximately 17% greater than the CuO/Al composition.

As was the case with the traditional thermite compositions, the thermite AM feedstocks all exhibited high thermal stability with Temperature of Ignition (T of I) values greater than 400 °C.

Table 4: Sensitiveness data for the thermite compositions

	Impact [F of I]	Av. Gas Output [mL]	BAM Friction [N]	ESD [J]	T of I [°C]
CuO/Al	60	0.10	>360	0.045	>400
PMMA/CuO/Al	70	0.25	>360	4.5	>400
PLA/CuO/Al	70	0.20	>360	4.5	>400
Bi_2O_3/Al	40	0.12	168	0.045	>400
PMMA/Bi_2O_3/Al	80	0.12	>360	0.45	>400
PLA/Bi_2O_3/Al	70	0.13	>360	0.45	>400

The PMMA/CuO/Al and PLA/CuO/Al formulations also showed no measurable change to the friction sensitiveness, indicating no adverse increases by the inclusion of either binder.

A marginal decrease in impact sensitiveness was observed in both PMMA/CuO/Al and PLA/CuO/Al formulations, although the average volume of gas produced during testing at least doubled compared to the traditional CuO/Al thermite. Of greatest significance is the reduction of the ESD sensitiveness by two orders of magnitude (0.045 to 4.5 J) by both AM thermite feedstocks compared to the traditional thermite. This result demonstrates the potentially significant improvement in the safe handling of these formulations through the reduction in ESD sensitiveness.

The Bi_2O_3/Al AM feedstock formulations showed significant improvements in overall sensitiveness compared to the traditional thermite formulation. Both AM formulations significantly decreased the friction sensitiveness of the traditional Bi_2O_3/Al thermite from 168 N of force to >360 N with no observable ignition event. The inclusion of PMMA in the formulation doubles the F of I of the traditional Bi_2O_3/Al thermite from 40 to 80. This poses a significant reduction in impact sensitiveness. The PLA/Bi_2O_3/Al displayed higher impact sensitiveness compared to the PMMA/Bi_2O_3/Al, with an F of I of 70. This remains, however, a significant improvement compared to the neat Bi_2O_3/Al thermite F of I. The inclusion of both binders had no apparent impact on the volume of gas produced during an ignition event. As was the case for the CuO/Al thermite AM feedstock formulations, the combination of both binders with Bi_2O_3/Al resulted in a reduction of the ESD sensitiveness from 0.045 J to 0.45 J. Although this not as pronounced as the decrease in ESD sensitiveness for the CuO/Al formulations, these results still suggest potentially significant improvements in the safe handling of these formulations.

3.7. Ignition

Initial formulations containing PMMA or PLA with either CuO/Al (80:20) or Bi_2O_3/Al (90:10) thermite, were prepared at a solid loading of 90 wt% for ignition testing. Still images of the resulting outputs are shown in Figure 6. All formulations were able to be readily ignited by the application of a flame, either from a safety match or a blow torch.

Propagation of the combustion wave for the PMMA/CuO/Al formulation was inconsistent, with the composition producing sparks, popping and flashing bright white light. Quenching of the reaction was also observed before the composition was completely consumed, requiring extended application of a flame to re- ignite the remaining composition. This indicates quenching of the reaction via insufficient heat transfer along the combustion front, potentially due to too much heat being lost to the surrounding environment or poor contact between the fuel and oxidiser particles in the PMMA matrix.

In contrast, the PLA/CuO/Al formulation burned evenly to completion, producing white light and minimal smoke. A reason for this increase in the reactivity of the PLA-based formulation could be attributed to the more positive oxygen balance of PLA (-133.2%) compared to that of PMMA (-191.8%), calculated based on the monomer unit of each polymer with complete oxidation to CO_2. Due to the higher (i.e. more positive) oxygen balance of PLA, less oxygen is required to complete the combustion of the binder, thus ensuring that more oxygen is available to react with the aluminium fuel, when compared to that of the PMMA system. Similar trends have been previously reported in other pyrotechnic systems using non-energetic binders [20]. This suggests that the PLA/CuO/Al formulation has significant potential for future development of thermite AM feedstock from a performance perspective.

Both the PMMA/Bi_2O_3/Al and PLA/Bi_2O_3/Al formulations were found to undergo sustained combustion. The PMMA/Bi_2O_3/Al formulation propagated with an orange flame, producing small sparks for the duration of the burn and a significant amount of smoke. Despite the heterogeneous nature of the PLA/Bi_2O_3/Al formulation, as evident by the bright yellow Bi_2O_3 agglomerates in an otherwise light grey binder matrix; the formulation was able to be ignited. After some initial sparks, this formulation propagated with an orange flame, giving off a considerable amount of smoke.

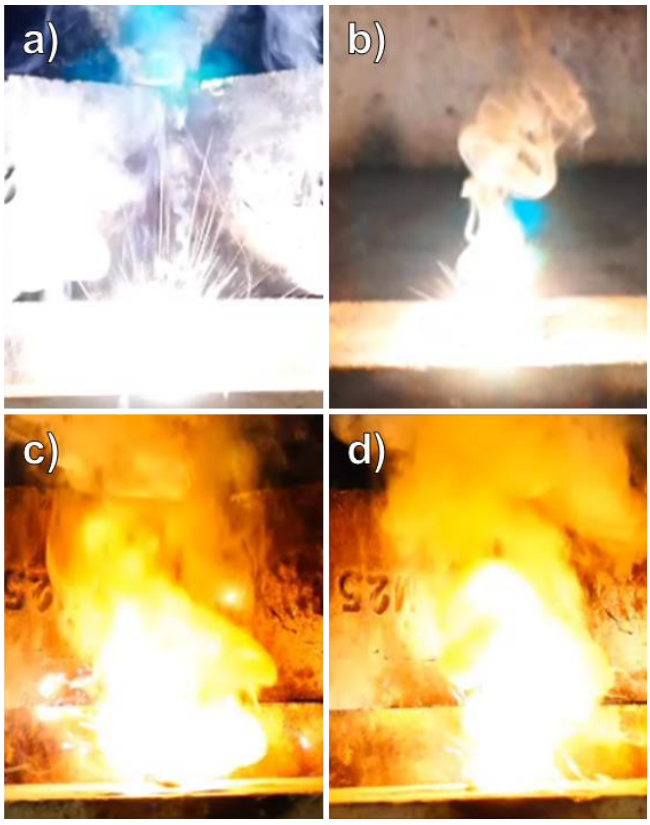

Figure 6: Still image of the flame ignition test of a) PMMA/CuO/Al (1.0 g); b) PLA/CuO/Al (0.5 g); c) PMMA/Bi_2O_3/Al (0.8 g) and d) PLA/Bi_2O_3/Al (0.8 g) thermite AM formulations

4. Conclusions

This work compared the ignition sensitiveness of potential thermite AM feedstocks to traditional thermite compositions, with the aim of identifying potential improvements to the safe handling of thermites. The formulations were based on either CuO/Al or Bi_2O_3/Al thermites combined at 90 wt% with either PLA or PMMA binder. Ignition of each thermite AM feedstock was readily achievable through the application of thermal stimuli. It was found that these formulations are significantly less sensitive to processing and handling stimuli than the traditional thermite compositions, especially to ESD. The potential for the preparation of inert feedstocks for point-of-printing energetic material production is also possible with high solids loaded (90 wt%) binder matrices. This indicates that the utilisation of such pyrotechnic feedstocks for AM technologies may provide significant safety advantages over traditional production methods.

5. Future Work

Work investigating the rheological properties of additive manufacturing feedstocks, potential utilisation of additives and further optimisation of formulations is ongoing as this emerging technology continues to change the landscape of energetic material production.

6. Acknowledgements

The authors wish to thank Craig Wall, Joel Huf and Mark Mitchell for their assistance with sensitiveness testing. Phil Davies, Chad Prior and Andrew Hart are thanked for helpful discussions and for reviewing this manuscript.

7. Symbols and Abbreviations

T_{ad}	Adiabatic reaction temperature
AM	Additive Manufacturing
Al	Aluminium
Bi_2O_3	Bismuth(III) oxide
CuO	Copper(II) oxide
T_d	Decomposition temperature
ESD	Electrostatic discharge
F of I	Figure of Insensitiveness
FDM	Fused Deposition Modelling
T_m	Melting point
PLA	Polylactic Acid
PMMA	Polymethyl Methacrylate
RDX	Cyclotrimethylenetrinitramine
SEM	Scanning Electron Microscopy
SDT	Simultaneous Differential Thermal Analysis
T of I	Temperature of Ignition
V_R	Volume of reaction-generated gas

8. References

1. Shidlovskiy, A. A. (1997) *Principles of Pyrotechnics*, American Fireworks News
2. Fischer, S. and Grubelich, M. (1996) A survey of combustible metals, thermites, and intermetallics for pyrotechnic applications. In: *32nd AIAA/ASME/SAE/ASEE Joint Propulsion Conference and Exhibit*, Lake Buena Vista, Florida, USA
3. Conkling, J. A. and Mocella, C. J. (2011) *Chemistry of Pyrotechnics: Basic Principles and Theory, Second Edition*. Florida, USA, CRC Press
4. Dolman, B., et al. (2018) Advanced munitions: 3D printed firepower. In: *International Conference on Science and Innovation for Land Power 2018 (ICSILP 2018)*, Adelaide, SA: 6 September 2018, Defence Science and Technology Group
5. Gonzalez-Gutierrez, J., et al. (2018) Additive Manufacturing of Metallic and Ceramic Components by the Material Extrusion of Highly-Filled Polymers: A Review and Future Perspectives. *Materials (Basel)* **11** (5) May 18
6. (2010) *Standard Terminology for Additive Manufacturing Technologies*. ASTM
7. Muravyev, N. V., et al. (2019) Progress in Additive Manufacturing of Energetic Materials: Creating the Reactive Microstructures with High Potential of Applications. *Propellants, Explosives, Pyrotechnics*
8. Smit, K. J., Morgan, M. and Pietrobon, R. (2019) Pyrotechnic Films Based on Thermites Covered with PVC. *Propellants, Explosives, Pyrotechnics* **44** (1) 37-40
9. Wang, X., et al. (2017) 3D printing of polymer matrix composites: A review and prospective. *Composites Part B: Engineering* **110** 442-458
10. Bale, C. W., et al. *FactSage, version 7.0, Thermfact and GTT-Technologies*. (2015) [Accessed September 2016]; Available from: http://www.spencergroupintl.com.
11. Energetic Materials Testing and Assessment Policy Committee (2007) Manual of Tests, Issue One. In. UK, United Kingdom Ministry of Defence 68
12. Standardization Agreement STANAG 4147 (2004) *Chemical Compatibility of Ammunition Components with Explosives and Propellants (Non-Nuclear Application)*. NATO
13. Lafontaine, E. and Comet, M. (2016) *Nanothermites*, Wiley

14. Mohan, N., et al. (2017) A review on composite materials and process parameters optimisation for the fused deposition modelling process. *Virtual and Physical Prototyping* **12** (1) 47-59
15. Salem Bala, A., bin Wahab, S. and binti Ahmad, M. (2016) Elements and Materials Improve the FDM Products: A Review. *Advanced Engineering Forum* **16** 33-51
16. Laureto, J., et al. (2017) Thermal properties of 3-D printed polylactic acid-metal composites. *Progress in Additive Manufacturing* **2** (1-2) 57-71
17. Ahn, B. Y., et al. (2010) Printed origami structures. *Adv Mater* **22** (20) May 25 2251-4
18. Jakus, A. E., et al. (2015) Metallic Printing: Metallic Architectures from 3D-Printed Powder-Based Liquid Inks. *Advanced Functional Materials* **25** (45) 7099-7099
19. Clark, B., et al. (2017) 3D processing and characterization of acrylonitrile butadiene styrene (ABS) energetic thin films. *Journal of Materials Science* **52** (2) 993-1004
20. Sabatini, J. J., et al. (2011) An Examination of Binder Systems and Their Influences on Burn Rates of High-Nitrogen Containing Formulations. *Propellants, Explosives, Pyrotechnics* **36** (2) 145-150
21. Zeng, W. R., Li, S. F. and K., C. W. (2002) Review on Chemical Reactions of Burning Poly(methyl methacrylate) PMMA. *Journal of Fire Science* **20** 40-433
22. Lautenberger, C. and Fernandez-Pello, C. (2008) Pyrolysis modeling, thermal decomposition, and transport processes in combustible solids. In: Faghri, M. and Sundén, B. (eds.) *Transport Phenomena in Fires*. Vol. 31. Southampton, Boston, WIT Press 209-259
23. Ute, K., Miyatake, N. and Hatada, K. (1995) Glass transition temperature and melting temperature of uniform isotactic and syndiotactic poly(methyl methacrylate)s from 13mer to 50mer. *Polymer* **36** (7) 1995/03/01/ 1415-1419
24. Valandro, S. R., et al. (2013) Thermal properties of poly (methyl methacrylate)/organomodified montmorillonite nanocomposites obtained by in situ photopolymerization. *Materials Research* **17** (1) 265-270
25. Osuntokun, J. and Ajibade, P. A. (2016) Structural and Thermal Studies of ZnS and CdS Nanoparticles in Polymer Matrices. *Journal of Nanomaterials* **2016** 1-14
26. Rymuszka, D., et al. (2017) Wettability and thermal analysis of hydrophobic poly(methyl methacrylate)/silica nanocomposites. *Adsorption Science & Technology* **35** (5-6) 560-571
27. Holló, B. B., et al. (2014) Determination of natural rubber/poly(methyl methacrylate) blend composition by TG/DSC technique. *Journal of Thermal Analysis and Calorimetry* **119** (2) 1131-1137